

锑烯纳米层片用于活体肿瘤原位光声成像

于静文¹, 王秀翊^{1*}, 冯金超², 张娜², 王璞¹

¹北京市激光应用技术工程技术研究中心, 北京工业大学激光工程研究院,

跨尺度激光成型制造技术教育部重点实验室, 北京 100124;

²北京工业大学信息与通信工程学院, 北京 100124

摘要 光声成像作为一种新型的生物医学成像技术,其成像过程结合了光学成像的高分辨率以及声学成像的深层组织穿透性能,突破了传统生物医学成像的“软极限”。然而,大多数的肿瘤,尤其是在早期阶段,并无明显的光声对比度,因此,开发出有效的外源性光声成像造影剂至关重要。基于此,研究了一种新型二维材料——锑烯纳米层片(AMNFs),它在 300~900 nm 波段范围内具有较好的光学吸收性,且具备优异的光热转换效率和光声性能。用此材料作为对比剂,可以实现活体小鼠体内小肿瘤的高质量光声成像。

关键词 生物光学; 光声成像; 造影剂; 二维材料; 肿瘤成像

中图分类号 O437

文献标志码 A

doi: 10.3788/CJL202047.0207033

Antimonene Nanoflakes as a Photoacoustic Imaging Contrast Agent for Tumor *in vivo* Imaging

Yu Jingwen¹, Wang Xiuhong^{1*}, Feng Jinchao², Zhang Na², Wang Pu¹

¹Beijing Engineering Research Center of Laser Technology, Institute of Laser Engineering of Beijing University of Technology, Key Laboratory of Trans-Scale Laser Manufacturing Technology, Ministry of Education, Beijing 100124, China;

²College of Electronic Information and Control Engineering, Beijing University of Technology, Beijing, 100124, China

Abstract Photoacoustic imaging, a novel biomedical imaging technique that combines the advantages of optical imaging and acoustic imaging, offers high-resolution biological tissue imaging to facilitate the observation of deeper imaging sites. In other words, it breaks the “soft limit” of conventional optical bioimaging techniques. However, many diseases, especially in the early stage, present no obvious photoacoustic contrast; therefore, it is crucial to identify effective exogenous photoacoustic contrast agents. Here we introduce a novel two-dimensional material, antimonene nanoflakes (AMNFs), which demonstrates great optical absorption from 300 nm to 900 nm as well as excellent photothermal conversion efficiency and photoacoustic performance. This material is expected to be useful as a contrast agent, helping to achieve excellent photoacoustic imaging of ultra-small tumors *in vivo*.

Key words biological optics; photoacoustic imaging; contrast agent; two-dimensional materials; tumor imaging

OCIS codes 170.6280; 040.5160; 130.6010; 140.3945

1 引言

生物医学成像^[1-6]作为生物医学^[7-9]研究领域的关键技术一直受到研究人员的广泛关注。不同的成像手段,如荧光分子成像^[10-15]、扩散光学层析成像^[16-22]、X-ray 层析成像^[23-25]及常用的超声成

像^[26-27],在分辨率、对比度及成像深度上各有优劣。光声成像^[28]作为一种非侵入且非电离式的新型生物医学成像手段,成功地结合了纯光学成像的高分辨率和纯声学成像的深层组织穿透性能,利用声子在生物组织内部单位扩散路径上所产生的散射比光子散射小三个数量级这一优势^[29],从原理上成功地

收稿日期: 2019-10-21; 修回日期: 2019-11-27; 录用日期: 2019-12-16

基金项目: 国家自然科学基金(61527822)、国家重点研发计划(2017YFB0405201)、北京市自然科学基金(4192013, L182011)

* E-mail: wxh2012@bjut.edu.cn

规避了传统光学成像的成像深度^[30-33]只能达到1 mm这一“软极限”^[34-35]。光声成像过程主要依赖于光声效应,成像系统中的脉冲光源到达成像部位后,其所携带的光子能量被成像部位的内源/外源性造影剂所吸收,成像部位发生瞬态热膨胀导致成像组织或器官产生微小的弹性形变,从而产生高频超声波^[36],利用超声波探测器接收这些信号,就可实现对活体生物较深部位从组织到器官不同层面^[29]的高质量成像。这一技术发展过程中所面临的最大局限性在于,其成像效果很大程度上取决于外源性造影剂^[37]的性能。因此,开发出适用于体内高效光声成像的外源性造影剂至关重要。与此同时,二维材料无论是在材料科学领域^[38]还是在纳米医学范畴^[9,39-43]都是最为活跃的研究热点。2004年,Geim小组成功制备得到了单层石墨结构——石墨烯^[44-46],石墨烯的进一步研究结果表明,它除了具备基本的科学研究价值外,还在通信、储能及催化传感^[47]等领域具有潜在的应用前景。然而,石墨烯是一种零带隙半金属材料,这大大限制了其在电子及光子^[48]领域的应用^[49]。然而,很快就有人预测,将二维六方氮化硼^[50](hBN)沉积在石墨烯上,所得的异质结构会产生层间带隙,这使得六方氮化硼一度成为研究的热点;此外,研究人员还发现过渡族金属的卤族化合物(TMDs)具有带隙大小随层厚可调的特性,进一步推动了半导体二维层状材料的研究进展。2006年,Li等^[51]制备得到了基于黑磷的高性能光电子设备,从此黑磷获得了广泛的关注。近十年来,作为二维材料的代表,黑磷^[52]在光电子领域和生物医学领域的表现都十分亮眼,然而它在水和大气环境中不稳定且极易降解,限制了它的进一步应用。因此,开发出性能更加优异的新型二维材料就变得更为迫切。此时,另一V族元素锑烯(antimonene)因具有类似于石墨烯的层状二维结构、极强的自旋轨道耦合特性^[38]而逐渐受到关注。少层锑烯是一种特殊结构的拓扑半金属^[53],具有优异的半导体性能^[54],在光电子领域有广阔的应用前景。在生物医学领域,与其他二维材料类似,锑烯纳米层片因具有大的表面积而可以作为药物的有效载体。

本文研究了锑烯用于光声成像的潜力。利用液相超声剥离法制备得到锑烯纳米层片(AMNFs),结合理论计算^[55]与实验测试,探索了锑烯纳米层片的光热转换效率及光声转换机制,并实现了对体内原位肿瘤的较高对比度光声造影成像。结果显示,锑烯纳米层片作为一种新型的无机纳米光声成像造影

剂,具有优异的造影效果及较高的生物医学兼容性,无任何明显的毒副作用,可经生物体内循环自行排出,是一种性能卓越且极具前景的光声成像造影剂。

2 实验材料及仪器设备

锑烯纳米层片的制备:取一定量的锑粉末分散于N-甲基吡咯烷酮(NMP)中,形成初始质量浓度为30 mg/mL的悬浊液,利用探针超声与液相超声相结合的方法,在冰浴条件下经循环超声(探针超声5 h-液相超声6 h-探针超声3 h,600 W)处理后再经离心机离心(3000 r/min,5 min),可得到少层锑烯纳米层片,去掉上清液后将沉淀物重新分散于超纯水或纯乙醇(99.9%)中。

锑烯纳米层片的修饰:为了使制备所得的锑烯纳米层片具备更加优异的分散性和生物兼容性,本文利用38.8 mmol/L的柠檬酸钠溶液对上述制备得到的锑烯纳米层片进行包覆修饰。按11.4 mg/mL的质量浓度将柠檬酸钠粉末溶解于去离子水中,然后将其与一定浓度的锑烯纳米层片水溶液在30 °C下混合,搅拌2 h,之后在离心机中以3000 r/min(3 min)的速度对样品进行离心处理,去掉上清液,将所得的沉淀重新分散在水溶液中以备后用。

细胞培养:将乳腺癌细胞MCF-7、人胚胎肾细胞293T及人乳腺导管癌细胞T-47D放于DMEM培养基中,在37 °C、5%(体积分数)的CO₂气体中孵育。

小鼠肿瘤模型:乳腺癌细胞MCF-7常规培养。收集约 1×10^7 个MCF-7细胞,皮下接种于BALB/c裸鼠中,观察肿瘤的生长情况。约1~2周后,在实体肿瘤大小为0.1~0.3 cm³时将该BALB/c裸鼠用作实验动物成像模型。

实验所用仪器:探针超声分散仪,液相超声清洗机,细胞培养箱,iThera Medical小动物活体多光谱光声断层扫描成像系统(MSOT)

3 实验结果与讨论

3.1 锑烯纳米层片的制备及性能表征

本文利用改进后的液相剥离方法^[56]制备锑烯纳米层片。分别用超纯水、乙醇及N-甲基吡咯烷酮作为分散剂,加入分散剂后的锑烯纳米层片水溶液经循环超声后,再利用离心机进行离心处理,后经多次清洗可制备得到不同层厚、不同片径大小的锑烯纳米层片。实验中发现,选用N-甲基吡咯烷酮作为

分散剂得到的产品最稳定、产率最高(约为 60%)。利用透射电子显微镜观察铈烯纳米层片形貌,发现实验制备得到的样品呈现不规则片状结构,其层片横向尺寸大都分布于 50~55 nm 范围内。利用原子力显微镜(AFM)测量得到其平均厚度为 25 nm。已知单层铈烯纳米层片的层间间距约为 0.4 nm^[55],分散于溶剂中时,其水合层厚约为 4 nm。由此可得

制备的铈烯纳米材料大约在 7 层左右。由于纳米材料尺寸较小,比表面积急剧下降,表面能量较高,处于不稳定状态,因而在溶液中极易团聚^[57],这会影晌后续的实验。为了避免团聚,本文采用 38.8 mmol/L (11.4 mg/mL) 的柠檬酸钠溶液修饰制备所得的铈烯纳米层片,使其可均匀稳定地分散于超纯水中。

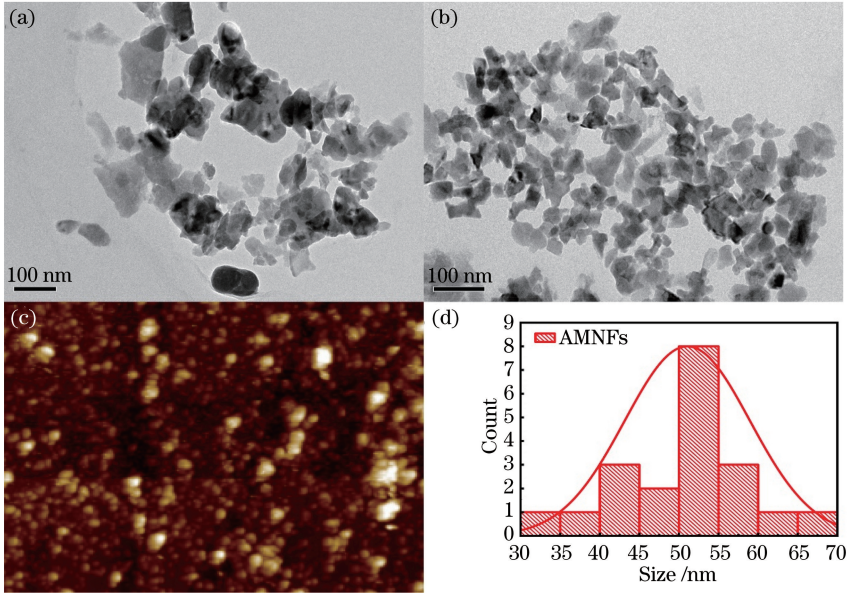


图 1 铈烯纳米层片的表征分析。(a)铈烯纳米层片的透射电镜图;(b)柠檬酸钠修饰的铈烯纳米层片的透射电镜图;(c)图 1(b)铈烯纳米层片的原子力显微镜图;(d)图 1(b)中均匀分散的大片径(50~55 nm)铈烯纳米层片的粒径分布
Fig. 1 Characterization of AMNFs. (a) Transmission electron micrograph(TEM) of AMNFs; (b) TEM of AMNFs modified with sodium citrate; (c) atomic force micrograph of AMNFs in Fig. 1 (b); (d) size distribution of uniformly dispersed large-scale(50~55 nm) AMNFs in Fig.1(b)

3.2 铈烯纳米层片的光热转换性能

光声成像的对比度并不依赖于组织的机械弹性性质^[58],而是取决于成像部位的光学性质,尤其是光学吸收。因而,铈烯纳米层片所具有的优异的光学吸收性能为其作为光声成像造影剂提供了契机。

由图 2(a)可见,铈烯纳米层片在 300~900 nm 的全波段范围内都具有较强的光学吸收特性,且随其浓度增大光学吸收性显著增强。基于此优异的光学吸收性能,本文进一步利用实验测得的数据结合理论计算^[59]得到了铈烯纳米层片的消光系数(ϵ)和光热转换效率(η)。近红外(NIR)窗口为 800 nm 时,铈烯纳米层片的消光系数高达 2.24×10^9 ,优于目前广泛使用的小分子及无机纳米光声成像造影剂。此外,作为光声造影剂性能的决定性因素,光热转换效率可经红外热成像仪探测得到,在 808 nm、2 W/cm² 的近红外激光照射下,铈烯纳米层片表现出了明显的温度变化,且其温度变化随样品浓度的增大

而显著提升。其中,经 808 nm 2 W/cm² 激光照射 5 min 后,质量浓度为 500 μ g/mL 的铈烯纳米层片的温度从 21 $^{\circ}$ C 升高至 101.5 $^{\circ}$ C,如图 2(b)所示。利用热成像实验测得的一系列数据进一步计算可得到 808 nm 光照下铈烯纳米层片的光热转换效率为 42.36%,为常用光声成像造影剂——金纳米棒^[60]($\eta=21\%$)的 2 倍左右。光热转换效率的计算式为

$$\eta = \frac{hA(T_{\max} - T_{\text{sur}}) - Q_{\text{dis}}}{I \cdot (1 - 10^{-A_{808}})}, \quad (1)$$

式中: h 为传热系数; A 为辐照受热材料的表面积; T_{\max} 为光照过程中材料所达到的最高温度; T_{sur} 为环境温度; Q_{dis} 为环境损耗能量; I 为入射光光强; A_{808} 为 808 nm 处材料的吸光度。

3.3 铈烯纳米层片的光声性能及其光声转换机制

光热转换效率越高越适合作为光声成像造影剂。但是决定一种材料光声转换性能的并不仅仅是其光热转换效率。在此,进一步研究了影响铈烯

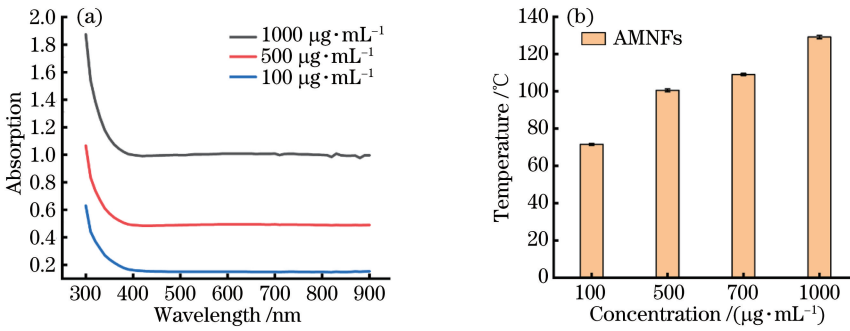


图 2 铈烯纳米层片的光学性质。(a) 不同浓度铈烯纳米层片的吸收光谱;(b) 铈烯纳米层片的光热转换性能

Fig. 2 Optical properties of AMNFs. (a) Absorption spectra of AMNFs with different concentration; (b) photothermal conversion performance of AMNFs

纳米层片光声转换机制的其他因素。首先,研究了不同浓度铈烯纳米层片的光声性能,如图 3(a)所示。由图 3 可知,不同于类似结构的其他层状二维材料(如石墨烯)^[61],铈烯纳米层片的光声信号随其浓度的增大而显著提升,500 $\mu\text{g}/\text{mL}$ 的铈烯纳米层片所产生的光声信号是相同条件下石墨烯的 4 倍。此外,调整实验过程中的制备参数(超声功率、超声时间、离心速度、离心时间),获得了横向尺寸分别约为 55 nm[图 1(b)]及 20 nm 的少层铈烯纳米层片。利用不同大小的铈烯纳米层片进行光声信号探测,得到 55 nm 铈烯纳米层片的光声信号明显优于小尺寸(20 nm)铈烯纳米层片,如图 3(c)所示。铈烯纳米材料的光声性能明显优于石墨烯的原因,以及材料尺寸对铈烯纳米材料

光声性能进一步的影响,解释如下。首先,相比于石墨烯等其他常见二维材料光声造影剂,铈烯纳米层片的热导率仅为 15.1 $\text{W}/(\text{m}\cdot\text{K})$ [石墨烯的热导率^[62]为 5300 $\text{W}/(\text{m}\cdot\text{K})$],其极低的热导率进一步使得铈烯纳米层片具有低的热扩散系数,从而较强的热封闭性使得铈烯纳米层片具有优异的光声信号;外源性光声成像造影剂在成像过程中所产生的光声信号强度主要取决于以下因素^[35-63]:样品尺寸、样品本身的热扩散系数和光学吸收率,其中较大尺寸的样品具有更长的热禁闭时间^[64],在此前提下,若采用更大脉宽的激光器即可在光声成像过程中提供更高的单脉冲激光能量,则此时片径较大的铈烯纳米层片能产生更强的光声效应。

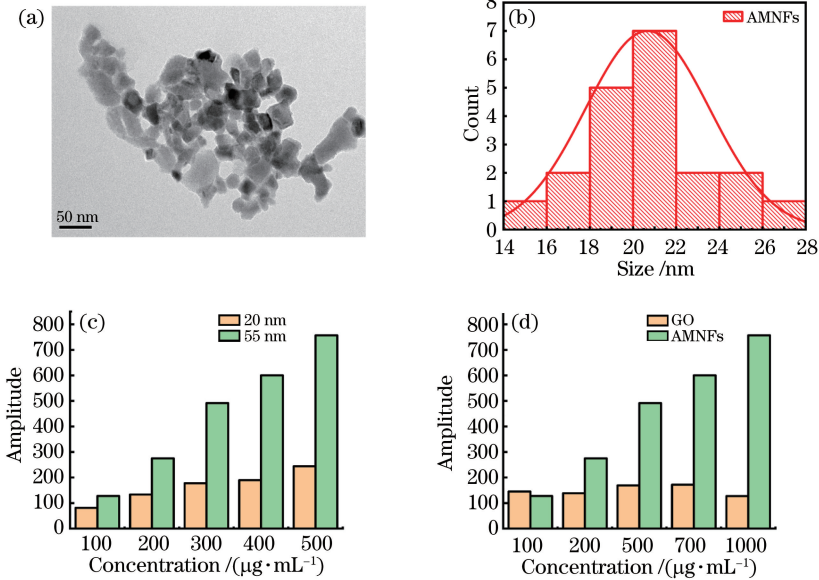


图 3 铈烯纳米层片(AMNFs)的光声性能。(a) 铈烯纳米层片透射电镜图;(b) 图 3(a) 铈烯纳米层片的粒径分布;

(c) 铈烯纳米层片在 808 nm 处的光声信号对比;(d) 铈烯纳米层片与氧化石墨烯在 808 nm 处的光声信号对比

Fig. 3 Photoacoustic performance of AMNFs. (a) TEM of AMNFs; (b) size distribution of AMNFs in Fig.3 (a); (c) photoacoustic signal of AMNFs at 808 nm; (d) photoacoustic signals of AMNFs and graphene oxide (GO) at 808 nm

3.4 活体肿瘤原位光声成像

铈烯纳米层片具有较高的光热转换效率、优异的光声造影效果,其表面经化学修饰后具有较好生物兼容性和分散性,因此本文利用铈烯纳米层片作为光声成像造影剂对乳腺癌细胞 MCF-7 荷瘤小鼠进行活体肿瘤原位光声成像。向小鼠体内注射 200 μL (3 mg/mL)的铈烯纳米材料,因为实体瘤的高通透性和滞留效应^[65],铈烯纳米材料会在肿瘤部位富集。分别利用 808 nm 和 680 nm 的激光源,在不同时间点对小鼠的肿瘤部位进行成像。分析成像结果后发现,注射 1 h 后,造影剂在肿瘤部位的富集量达到了最大,肿瘤部位成像对比度较高,能够对大小约为 100 mm^3 的肿瘤实现较高质量的光声成像,从而能够实现对较小肿瘤的检测,如图 4 所示。注

射后 48 h 内不同时间点的成像结果显示,肿瘤部位的光声信号强度随着时间的延长而逐渐减弱,在 24 h 时只有很少的材料残留在肿瘤部位,而在 48 h 时,肿瘤部分几乎无铈烯纳米层片残余。此外,本文还进行了如下体外细胞生物毒性实验:先将不同质量浓度的铈烯纳米层片(100, 200, 500, 700, 1000 $\mu\text{g}/\text{mL}$)与 5000 个乳腺癌细胞 MCF-7 共培养 24 h,再利用 Calcein-PI 对其进行双染,然后利用激光共聚焦显微镜观察,成像图如图 5 所示。由图 5 可知乳腺癌细胞仍具有较好的细胞活性,表明铈烯纳米层片并无明显的生物毒性。以上结果表明铈烯纳米层片作为一种外源性无机造影剂可实现肿瘤部位的特异性富集,具有较高生物兼容性且可随生物体的自身循环系统排出,无明显毒副作用。

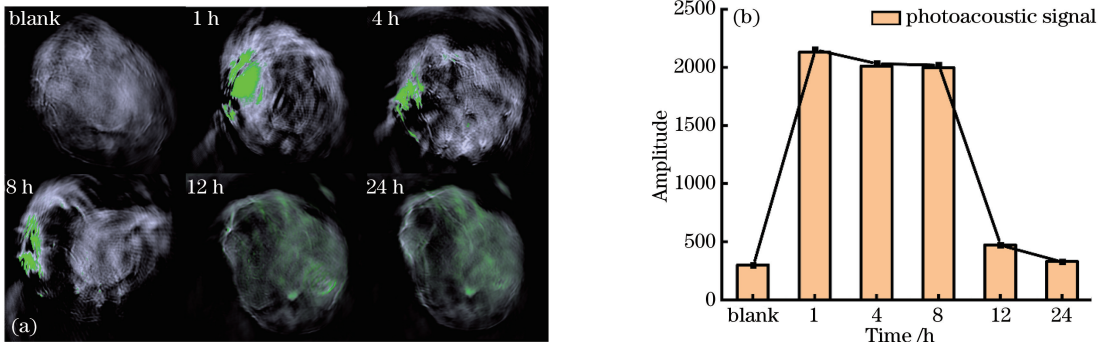


图 4 不同时间荷瘤小鼠原位光声成像。(a)注射 200 μL 3 mg/mL 的铈烯纳米层片后不同时刻小鼠肿瘤部位的原位光声成像;(b)注射 200 μL 3 mg/mL 铈烯纳米层片后不同时刻小鼠肿瘤部位的原位光声信号图
Fig. 4 Photoacoustic imaging of tumor site at various time. (a) Photoacoustic imaging of tumor site at various time after 200 μL 3 mg/mL AMNFs injection; (b) photoacoustic signal of the tumor site at various time after 200 μL 3 mg/mL AMNFs injection

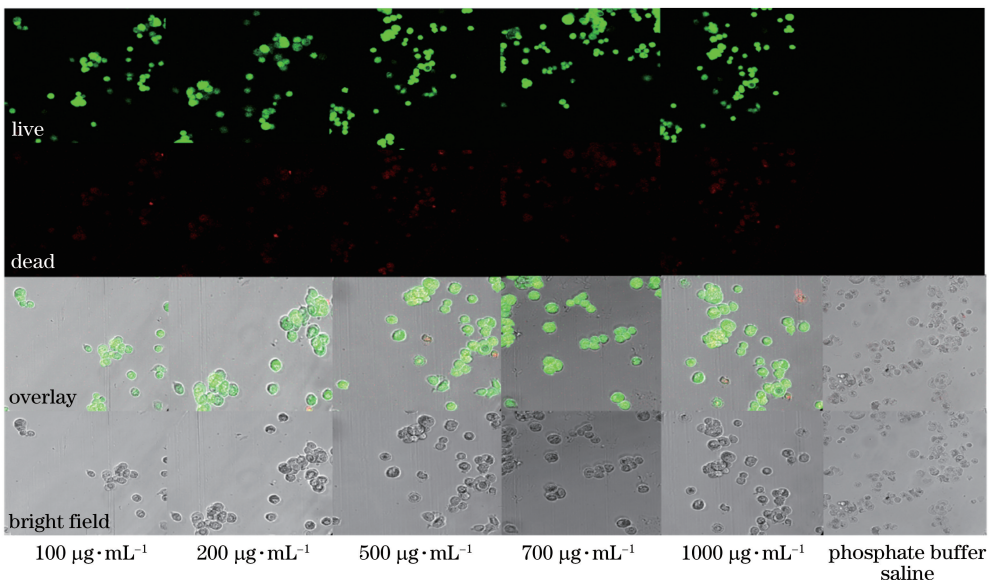


图 5 不同浓度的铈烯纳米层片与 MCF-7 细胞共培养 24 h 后的双染激光共聚焦成像图
Fig. 5 Laser confocal microscopy imaging of MCF-7 cells cultivated 24 h with AMNFs in various concentrations

4 结 论

利用循环超声液相剥离法制备得到少层铋烯纳米层片,在发掘其在 300~900 nm 全波段范围内优异光学吸收性能的基础上,本文进一步采用理论计算与实验数据相结合的研究方法,论证了铋烯纳米层片具有优异的光热转换效率及光声效应,可作为一种性能优异且极具前景的无机纳米光声成像造影剂,实现对乳腺癌荷瘤小鼠微型肿瘤的高质量原位活体成像,扩充了外源性光声成像造影剂的数据库且进一步开发了新型二维材料铋烯在生物医学成像领域的应用潜能。

参 考 文 献

- [1] Hahn M A, Singh A K, Sharma P, et al. Nanoparticles as contrast agents for *in-vivo* bioimaging: current status and future perspectives [J]. Analytical and Bioanalytical Chemistry, 2011, 399(1): 3-27.
- [2] Michalet X, Pinaud F F, Bentolila L A, et al. Quantum dots for live cells, *in vivo* imaging, and diagnostics[J]. Science, 2005, 307(5709): 538-544.
- [3] Freudiger C W, Min W, Saar B G, et al. Label-free biomedical imaging with high sensitivity by stimulated Raman scattering microscopy[J]. Science, 2008, 322(5909): 1857-1861.
- [4] Hong G S, Antaris A L, Dai H J. Near-infrared fluorophores for biomedical imaging [J]. Nature Biomedical Engineering, 2017, 1: 0010.
- [5] Hyun H, Owens E A, Wada H, et al. Cartilage-specific near-infrared fluorophores for biomedical imaging [J]. Angewandte Chemie International Edition, 2015, 54(30): 8648-8652.
- [6] Hyun H, Wada H, Bao K, et al. Phosphonated near-infrared fluorophores for biomedical imaging of bone [J]. Angewandte Chemie International Edition, 2014, 53(40): 10668-10672.
- [7] Giljohann D A, Seferos D S, Daniel W L, et al. Gold nanoparticles for biology and medicine [J]. Angewandte Chemie International Edition, 2010, 49(19): 3280-3294.
- [8] Gupta A K, Gupta M. Synthesis and surface engineering of iron oxide nanoparticles for biomedical applications[J]. Biomaterials, 2005, 26(18): 3995-4021.
- [9] Roca G, Costo R, Rebolledo F, et al. Progress in the preparation of magnetic nanoparticles for applications in biomedicine [J]. Journal of Physics D: Applied Physics, 2009, 42(22): 224002.
- [10] Hell S W, Wichmann J. Breaking the diffraction resolution limit by stimulated emission: stimulated-emission-depletion fluorescence microscopy [J]. Optics Letters, 1994, 19(11): 780-782.
- [11] Larson D R, Zipfel W R, Williams R M, et al. Water-soluble quantum dots for multiphoton fluorescence imaging *in vivo* [J]. Science, 2003, 300(5624): 1434-1436.
- [12] Dutta A, Pal G, Mitra K, et al. Fluorescence life time imaging from neurons and subcellular components during low intensity laser therapy using fiber-optic nano-probes [J]. Laser in Surgery and Medicine, 2006, 38: 11-11.
- [13] Flusberg B A, Cocker E D, Piyawattanametha W, et al. Fiber-optic fluorescence imaging [J]. Nature Methods, 2005, 2(12): 941-950.
- [14] Talley C E, Cooksey G A, Dunn R C. High resolution fluorescence imaging with cantilevered near-field fiber optic probes [J]. Applied Physics Letters, 1996, 69(25): 3809-3811.
- [15] Chatterjee D, Rufaihah A, Zhang Y. Upconversion fluorescence imaging of cells and small animals using lanthanide doped nanocrystals [J]. Biomaterials, 2008, 29(7): 937-943.
- [16] Xiong Q Z, Wang N S, Liu X Y, et al. Constrained polarization evolution simplifies depth-resolved retardation measurements with polarization-sensitive optical coherence tomography[J]. Biomedical Optics Express, 2019, 10(10): 5207-5222.
- [17] Correia T, Aguirre J, Sisniega A, et al. Split operator method for fluorescence diffuse optical tomography using anisotropic diffusion regularisation with prior anatomical information [J]. Biomedical Optics Express, 2011, 2(9): 2632-2648.
- [18] Correia T, Koch M, Ale A, et al. Patch-based anisotropic diffusion scheme for fluorescence diffuse optical tomography: part 2: image reconstruction [J]. Physics in Medicine and Biology, 2016, 61(4): 1452-1475.
- [19] Gaiind V, Tsai H R, Webb K J, et al. Small animal optical diffusion tomography with targeted fluorescence [J]. Journal of the Optical Society of America A, 2013, 30(6): 1146-1154.
- [20] Milstein A B, Oh S, Webb K J, et al. Fluorescence optical diffusion tomography [J]. Applied Optics, 2003, 42(16): 3081-3094.
- [21] Milstein A B, Stott J J, Oh S, et al. Fluorescence optical diffusion tomography using multiple-frequency data[J]. Journal of the Optical Society of America A, 2004, 21(6): 1035-1049.
- [22] Milstein A B, Webb K J, Bouman C A. Estimation

- of kinetic model parameters in fluorescence optical diffusion tomography [J]. Journal of the Optical Society of America A, 2005, 22(7): 1357-1368.
- [23] Pfeiffer F, Weitkamp T, Bunk O, et al. Phase retrieval and differential phase-contrast imaging with low-brilliance X-ray sources [J]. Nature Physics, 2006, 2(4): 258-261.
- [24] Wang L B, Frost J D, Lai J S. Three-dimensional digital representation of granular material microstructure from X-ray tomography imaging [J]. Journal of Computing in Civil Engineering, 2004, 18 (1): 28-35.
- [25] Kim D, Park S, Lee J H, et al. Antibiofouling polymer-coated gold nanoparticles as a contrast agent for *in vivo* X-ray computed tomography imaging [J]. Nanomedicine: Nanotechnology, Biology and Medicine, 2007, 3(4): 352.
- [26] Wei K, Jayaweera A R, Firoozan S, et al. Quantification of myocardial blood flow with ultrasound-induced destruction of microbubbles administered as a constant venous infusion [J]. Circulation, 1998, 97(5): 473-483.
- [27] Yang K, Zhang S, Zhang G X, et al. Graphene in mice: ultrahigh *in vivo* tumor uptake and efficient photothermal therapy [J]. Nano Letters, 2010, 10 (9): 3318-3323.
- [28] Li C H, Wang L H V. Photoacoustic tomography and sensing in biomedicine [J]. Physics in Medicine and Biology, 2009, 54(19): R59-R97.
- [29] Wang L H V, Hu S. Photoacoustic tomography: *in vivo* imaging from organelles to organs [J]. Science, 2012, 335(6075): 1458-1462.
- [30] Li H, Xia X Y, Chen T A, et al. Applications of two-photon excitation fluorescence lifetime imaging in tumor diagnosis [J]. Chinese Journal of Lasers, 2018, 45(2): 0207010.
李慧, 夏先园, 陈廷爱, 等. 双光子荧光寿命成像在肿瘤诊断研究中的应用 [J]. 中国激光, 2018, 45 (2): 0207010.
- [31] Lin H X, Zuo N, Zhuo S M, et al. Application of multiphoton microscopy in disease diagnosis [J]. Chinese Journal of Lasers, 2018, 45(2): 0207014.
林宏心, 左宁, 卓双木, 等. 多光子显微技术在医学诊断中的应用 [J]. 中国激光, 2018, 45 (2): 0207014.
- [32] Liu L X, Li M Z, Zhao Z G, et al. Recent advances of hyperspectral imaging application in biomedicine [J]. Chinese Journal of Lasers, 2018, 45 (2): 0207017
刘立新, 李梦珠, 赵志刚, 等. 高光谱成像技术在生物医学中的应用进展 [J]. 中国激光, 2018, 45(2): 0207017.
- [33] Chen Y, Wang L W, Song J. Multifunctional nanophotonics technology for precise biomedical applications [J]. Chinese Journal of Lasers, 2018, 45 (3): 0307003.
陈越, 王璐玮, 宋军. 面向精准化生物医学的多功能纳米光子学技术 [J]. 中国激光, 2018, 45 (3): 0307003.
- [34] Zhang J Y, Xie W M, Zeng Z P. Recent progress in photoacoustic imaging technology [J]. Chinese Optics, 2011, 4(2): 111-117.
张建英, 谢文明, 曾志平. 光声成像技术的最新进展 [J]. 中国光学, 2011, 4(2): 111-117.
- [35] Wang L V. Multiscale photoacoustic microscopy and computed tomography [J]. Nature Photonics, 2009, 3(9): 503-509.
- [36] Miao S F, Yang H, Huang Y H, et al. Research progresses of photoacoustic imaging [J]. Chinese Optics, 2015, 8(5): 699-713
苗少峰, 杨虹, 黄远辉, 等. 光声成像研究进展 [J]. 中国光学, 2015, 8(5): 699-713.
- [37] Luke G P, Yeager D, Emelianov S Y. Biomedical applications of photoacoustic imaging with exogenous contrast agents [J]. Annals of Biomedical Engineering, 2012, 40(2): 422-437.
- [38] Pumera M, Sofer Z. 2D monoelemental arsenene, antimonene, and bismuthene: beyond black phosphorus [J]. Advanced Materials, 2017, 29(21): 1605299.
- [39] Moghimi S M, Hunter A C, Murray J C. Nanomedicine: current status and future prospects [J]. The FASEB Journal, 2005, 19(3): 311-330.
- [40] Ferrari M. Cancer nanotechnology: opportunities and challenges [J]. Nature Reviews Cancer, 2005, 5(3): 161-171.
- [41] Horcajada P, Chalati T, Serre C, et al. Porous metal-organic-framework nanoscale carriers as a potential platform for drug delivery and imaging [J]. Nature materials, 2010, 9(2): 172-178.
- [42] Farokhzad O C, Cheng J, Teplý B A, et al. Targeted nanoparticle-aptamer bioconjugates for cancer chemotherapy *in vivo* [J]. Proceedings of the National Academy of Sciences, 2006, 103(16): 6315-6320.
- [43] Cameron D J A, Shaver M P. Aliphatic polyester polymer stars: synthesis, properties and applications in biomedicine and nanotechnology [J]. Chemical Society Reviews, 2011, 40(3): 1761-1776.
- [44] Li D, Kaner R B. Materials science: graphene-based materials [J]. Science, 2008, 320(5880): 1170-1171.
- [45] Stankovich S, Dikin D A, Dommett G H B, et al.

- Graphene-based composite materials [J]. *Nature*, 2006, 442(7100): 282-286
- [46] Son Y W, Cohen M L, Louie S G. Half-metallic graphene nanoribbons [J]. *Nature*, 2006, 444(7117): 347-349.
- [47] Bunch J S, van der Zande A M, Verbridge S S, et al. Electromechanical resonators from graphene sheets [J]. *Science*, 2007, 315(5811): 490-493.
- [48] Bonaccorso F, Sun Z, Hasan T, et al. Graphene photonics and optoelectronics [J]. *Nature Photonics*, 2010, 4(9): 611-622.
- [49] Vakil A, Engheta N. Transformation optics using graphene [J]. *Science*, 2011, 332(6035): 1291-1294.
- [50] Giovannetti G, Khomyakov P A, Brocks G, et al. Substrate-induced band gap in graphene on hexagonal boron nitride: *Ab initio* density functional calculations [J]. *Physical Review B*, 2007, 76(7): 073103.
- [51] Li L K, Yu Y J, Ge Q Q, et al. Black phosphorus field-effect transistors [J]. *Nature Nanotechnology*, 2014, 9(5): 372-377.
- [52] Kou L Z, Chen C F, Smith S C. Phosphorene: fabrication, properties, and applications [J]. *The Journal of Physical Chemistry Letters*, 2015, 6(14): 2794-2805.
- [53] Ji J, Song X, Liu J, et al. Two-dimensional antimonene single crystals grown by van der Waals epitaxy [J]. *Nature Communications*, 2016, 7: 13352.
- [54] Zhang S L, Yan Z, Li Y F, et al. Atomically thin arsenene and antimonene: semimetal-semiconductor and indirect-direct band-gap transitions [J]. *Angewandte Chemie International Edition*, 2015, 54(10): 3112-3115.
- [55] Ares P, Aguilar-Galindo F, Rodríguez-San-Miguel D, et al. Antimonene: mechanical isolation of highly stable antimonene under ambient conditions [J]. *Advanced Materials*, 2016, 28(30): 6515.
- [56] Gibaja C, Rodríguez-San-Miguel D, Ares P, et al. Few-layer antimonene by liquid-phase exfoliation [J]. *Angewandte Chemie International Edition*, 2016, 55(46): 14345-14349.
- [57] Keller A A, Wang H T, Zhou D X, et al. Stability and aggregation of metal oxide nanoparticles in natural aqueous matrices [J]. *Environmental Science & Technology*, 2010, 44(6): 1962-1967.
- [58] Yang S H, Yin G Z. Photoacoustic angiography for mouse brain cortex using near-infrared light [J]. *Acta Physica Sinica*, 2009, 58(7): 4760-4765.
杨思华, 阴广志. 利用近红外光激发的光声血管造影成像 [J]. *物理学报*, 2009, 58(7): 4760-4765.
- [59] Jain P K, Huang X H, El-Sayed I H, et al. Noble metals on the nanoscale: optical and photothermal properties and some applications in imaging, sensing, biology, and medicine [J]. *Accounts of Chemical Research*, 2008, 41(12): 1578-1586.
- [60] Agarwal A, Huang S W, O' Donnell M, et al. Targeted gold nanorod contrast agent for prostate cancer detection by photoacoustic imaging [J]. *Journal of Applied Physics*, 2007, 102(6): 064701.
- [61] Yang K, Hu L L, Ma X X, et al. Multimodal imaging guided photothermal therapy using functionalized graphene nanosheets anchored with magnetic nanoparticles [J]. *Advanced Materials*, 2012, 24(14): 1868-1872.
- [62] Zhou C Y, Zeng L, Ji L, et al. Research on the thermal conductivities of graphene and graphene based on composite materials [J]. *Development and Application of Materials*, 2010, 25(6): 94-100.
周春玉, 曾亮, 吉莉, 等. 石墨烯及其复合材料导热性能的研究现状 [J]. *材料开发与应用*, 2010, 25(6): 94-100.
- [63] Xu M H, Wang L V. Photoacoustic imaging in biomedicine [J]. *Review of Scientific Instruments*, 2006, 77(4): 041101.
- [64] Shi Y J, Xing D. Study on photoacoustic effect in nanoscale and photoacoustic conversion mechanism of nanoprobe [J]. *Chinese Journal of Lasers*, 2018, 45(2): 0207026.
石玉娇, 邢达. 纳米尺度下的光声效应及纳米探针光声转换机制研究 [J]. *中国激光*, 2018, 45(2): 0207026.
- [65] Fang J, Nakamura H, Maeda H. The EPR effect: unique features of tumor blood vessels for drug delivery, factors involved, and limitations and augmentation of the effect [J]. *Advanced Drug Delivery Reviews*, 2011, 63(3): 136-151.